

# Uncertainty in water transit time estimation with StorAge Selection functions and tracer data interpolation

Arianna Borriero<sup>1</sup>, Rohini Kumar<sup>2</sup>, Tam V. Nguyen<sup>1</sup>, Jan H. Fleckenstein<sup>1,3</sup>, and Stefanie R. Lutz<sup>4</sup>

<sup>1</sup>Department of Hydrogeology, Helmholtz-Centre for Environmental Research - UFZ, Leipzig, Germany

<sup>2</sup>Department of Computational Hydrosystems, Helmholtz-Centre for Environmental Research - UFZ, Leipzig, Germany

<sup>3</sup>Bayreuth Centre of Ecology and Environmental Research, University of Bayreuth, Bayreuth, Germany

<sup>4</sup>Copernicus Institute of Sustainable Development, Department of Environmental Sciences, Utrecht University, Utrecht, the Netherlands

**Correspondence:** Arianna Borriero (arianna.borriero@ufz.de)

**Abstract.** Transit time distributions (TTDs) of streamflow are useful descriptors for understanding flow and solute transport in catchments. Catchment-scale TTDs can be modeled using tracer data (e.g.,  $\delta^{18}\text{O}$ ; oxygen isotopes) in inflow and outflows, with StorAge Selection (SAS) functions. However, tracer data are often sparse in space and time, so they need to be interpolated to increase their spatio-temporal resolution. Moreover, SAS functions can be parameterized with different forms, but there is no general agreement on which one should be used. Both of these aspects induce uncertainty in the simulated TTDs, and the individual uncertainty sources as well as their combined effect have not been fully investigated. This study provides a comprehensive analysis of the TTD uncertainty resulting from twelve model setups obtained by combining different interpolation schemes for  $\delta^{18}\text{O}$  in precipitation, and distinct SAS functions. For each model setup, we found behavioral solutions with satisfactory model performances for instream  $\delta^{18}\text{O}$  (Kling-Gupta Efficiency,  $\text{KGE} > 0.55$ ). Differences in KGE values were statistically significant, thus showing the relevance of the chosen setup for simulating the TTDs. We found a large uncertainty in the simulated TTDs, represented by a large range of variability in the 95% confidence interval of the median transit time varying at the most between 259 and 1009 days across all tested setups. Uncertainty in TTDs was mainly associated with the temporal interpolation of  $\delta^{18}\text{O}$  in precipitation, the choice between time-variant and time-invariant SAS functions, flow conditions, and the use of non-spatially interpolated  $\delta^{18}\text{O}$  in precipitation. We discuss the implications of these results for the SAS framework, uncertainty characterization in TTD-based models, and the influence of the uncertainty for water quality and quantity studies.

## 1 Introduction

Understanding how catchments store and release water of different ages has significant implications for flow and solute transport as water ages encapsulate information about flowpaths characteristics (McGuire and McDonnell, 2006; Botter et al., 2011), contact time of solutes with the soil matrix (Benettin et al., 2015a; Hrachowitz et al., 2016), and vulnerability assessment (Kumar et al., 2020). This plays an important role for water resources protection and management, and requires a tool that can effectively describe catchment-scale transport processes (Rinaldo and Marani, 1987). The age of water in outflows is commonly

referred to as transit time (TT), i.e., the time elapsed between the entry of a water parcel into the catchment via precipitation and its exit via streamflow or evapotranspiration. Accordingly, the transit time distribution (TTD) describes the whole spectrum of the transit times in outflows (Botter et al., 2005; Van der Velde et al., 2010). Early studies have often assumed simplified steady-state transport models, resulting in time-invariant TTDs (Niemi, 1977; Rinaldo et al., 2006). However, experimental simulations showed that TTDs are time-variant due to the variability in meteorological forcing (Botter et al., 2010; Hrachowitz et al., 2010; Heidebüchel et al., 2020) and activation/deactivation of flowpaths in response to varying hydrologic conditions (Ambroise, 2004; Heidebüchel et al., 2013). Recent research has introduced new models for representing time-variant TTDs, for example allowing for the estimation of TTDs without making prior assumptions about their shape (Kirchner, 2019; Kim and Troch, 2022), or via parameterization of the StorAge Selections (SAS) functions (Rinaldo et al., 2015; Harman, 2019). SAS functions describe how catchments selectively remove water of different ages from storage for outflows, and have led to a new framework of non-stationary transport models based on water age, which have been successfully applied in various studies (Benettin et al., 2015b; Quéloz et al., 2015; Kim et al., 2016; Lutz et al., 2017; Wilusz et al., 2017; Nguyen et al., 2021).

Model-based TTDs are subjected to uncertainty, which limits their ability for decision support. In general, model prediction uncertainty stems from model inputs, structure, and parameters (Beven and Freer, 2001). As TTDs are not directly observable, conservative environmental tracers (e.g.,  $\delta^{18}\text{O}$ ; oxygen isotopes) in inflow and outflows are commonly used to infer water ages (Hrachowitz et al., 2013; Birkel and Soulsby, 2015; Stockinger et al., 2015). Long-term, high-frequency tracer data with appropriate spatial distribution is generally recommended for sufficient understanding of TTD dynamics across a wide range of fast and heterogeneous hydrological behaviors (Kirchner et al., 2004; Danesh-Yazdi et al., 2016; von Freyberg et al., 2017). Therefore, the lack of appropriate tracer data coverage can hamper our understanding of TTD dynamics at the desired resolution (McGuire and McDonnell, 2006). Additionally, uncertainty in the driving hydroclimatic fluxes such as precipitation, discharge, and evapotranspiration could propagate into the uncertainty of the modelling results. Further uncertainty emerges from the model structure due to the difficulty in representing physical processes because of our incomplete knowledge of complex reality (Ajami et al., 2007). Finally, specification of model parameters is also an important source of uncertainty (Beven, 2006; Kirchner, 2006), as the best-fit parameters may suffer from equifinality (Schoups et al., 2008).

A few studies have investigated the uncertainty in the estimated TTDs with SAS models. Danesh-Yazdi et al. (2018) and Jing et al. (2019) have analysed the effect of interactions between distinct flow domains, external forcing and recharge rate on resulting TTDs. Several works (Benettin et al., 2017; Wilusz et al., 2017; Rodriguez et al., 2018, 2021) have explored model parameter uncertainty, and suggested that additional types of tracers, data on physical characteristics of the catchment, and parsimonious parameterization may help to further reduce parametric uncertainty in the SAS models. More recently, Buzacott et al. (2020) investigated how gap-filling of the  $\delta^{18}\text{O}$  record in precipitation propagated uncertainty into the simulated mean water transit time (MTT), i.e., the average time it takes for water to leave the catchment (McDonnell et al., 2010).

Despite the studies cited above, there are other aspects particularly significant for SAS modelling causing uncertainty in the simulated TTDs, which have not yet been thoroughly investigated. First, isotope data are generally sparse globally in space and time (von Freyberg et al., 2022), due to laborious and costly sampling campaigns limited to well-equipped areas (Tetzlaff et al., 2018). As SAS models require continuous time series of input tracer data, different methods for temporal interpolation

could be used to reconstruct isotope values in precipitation; consequently, the interpolated input data are subject to uncertainty. Furthermore, the input data of SAS models are influenced by whether the tracer data in precipitation are collected at a single location within the catchment, or at multiple locations. In the latter scenario, there is a need to account for the spatial variability of tracer composition in precipitation, which is commonly done via spatial interpolation. Choosing data from one approach (i.e., tracer data from a single location) over the other (i.e., tracer data spatially interpolated based on multiple locations, including stations outside the catchment boundaries) can potentially result in different resulting TTDs. Finally, SAS functions, employed to model TTDs, must be parameterized and their functional forms need to be specified a-priori. Commonly used forms are the power law (Benettin et al., 2017; Asadollahi et al., 2020), beta (van der Velde et al., 2012; Drever and Hrachowitz, 2017) and gamma (Harman, 2015; Wilusz et al., 2017) distributions. However, there is no general agreement on which SAS function should be used since the hydrological processes that control the patterns and dynamics of the subsurface vary across catchments. Therefore, the most convenient approach is to simply rely on a specific parameterization over another, and estimate its parameters (Harman, 2015). All of these aspects, related to model input, structure and parameter, induce uncertainty in the simulated TTDs. To date, the role of these individual uncertainty sources and their combined effect on the modeled TTDs have not been adequately discussed.

This study bridges the aforementioned gaps by specifically exploring the combined effect of tracer data interpolation and model parameterizations on the simulated TTDs. We investigated TTD uncertainty using a SAS-based catchment-scale transport model applied to the Upper Selke catchment, Germany. We evaluated TTDs resulting from twelve model setups obtained by combining distinct interpolation techniques of  $\delta^{18}\text{O}$  in precipitation, and parameterizations of SAS functions. For each model setup, we searched for behavioral parameter sets (i.e., those providing acceptable predictions) based on model performance for instream  $\delta^{18}\text{O}$ , evaluated the sources of uncertainty and their combined effects, in the modeled TTDs. Overall, our results provide new insights into the uncertainty characterization of TTDs, particularly in the absence of high-frequency tracer data, and the use of SAS functions, as well as implications of TTDs uncertainty on water quantity and quality studies.

## 2 Study area and data

The Upper Selke catchment is located in the Harz Mountains in Saxony-Anhalt, central Germany (Fig. 1). The study site is part of the Bode region, an intensively monitored area within the TERENO (TERrestrial ENvironmental Observatories; Wollschläger et al., 2017) network. The catchment has a drainage area of 184 km<sup>2</sup>, the altitude ranges between 184 and 594 m above mean sea level, and the mean slope is 7.65%. Land use is dominated by forest (broadleaf, coniferous and mixed forest) and agricultural land (winter cereals, rapeseed and maize), representing 72% and 21% of the catchment, respectively. The soil is largely composed of cambisols and the underlying geology consists of schist and claystone, resulting in a predominance of relatively shallow flowpaths (Dupas et al., 2017; Yang, J. et al., 2018).

Daily hydroclimatic and monthly tracer data in the Upper Selke were available for the period between February 2013 and May 2015. Precipitation (P) was taken from the German weather service, while discharge (Q) and evapotranspiration (ET) were simulated data obtained from the mesoscale Hydrological Model (mHM; Samaniego et al., 2010; Kumar et al., 2013) since

continuous measurements were not available for the given outlet and period. A thorough evaluation of mHM performance for past measurements have been conducted in previous studies (Zink et al., 2017; Yang, X. et al., 2018; Nguyen et al., 2021). The average annual P, Q and ET are 703, 108, 596 mm, respectively. The area is characterized by high flow during November-May (average Q = 0.88 m<sup>3</sup>/s) and low flow during June-October (average Q = 0.42 m<sup>3</sup>/s). Evapotranspiration is higher in June (109 mm/month) and lower in December (10 mm/month). The average monthly temperature ranges from -0.7°C in January to 17°C in July. The  $\delta^{18}\text{O}$  values in precipitation ( $\delta^{18}\text{O}_P$ ) and in streamflow ( $\delta^{18}\text{O}_Q$ ) at monthly resolution were taken from Lutz et al. (2018), and are displayed in Fig. 2. Values of  $\delta^{18}\text{O}_P$  were used in the form of "raw" (i.e., values collected at the catchment outlet) and processed (i.e., values collected at multiple location and spatially interpolated using kriging) data (see Section 3.2 for more details). The variability in  $\delta^{18}\text{O}_P$  was larger than  $\delta^{18}\text{O}_Q$  (Fig. 2) because of the damping of the precipitation signal due to mixing and dispersion within the catchment. Temperature dependence caused more depleted (i.e., more negative)  $\delta^{18}\text{O}_P$  in winter than in summer (Fig. 2).

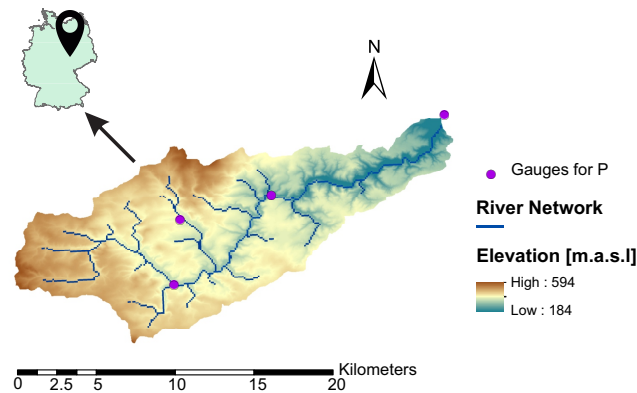


**Figure 1.** Upper Selke catchment with precipitation sampling points (purple dots), river network (blue lines), and elevation in meters above sea level as colored map; location of the Upper Selke catchment in Germany (upper left corner).

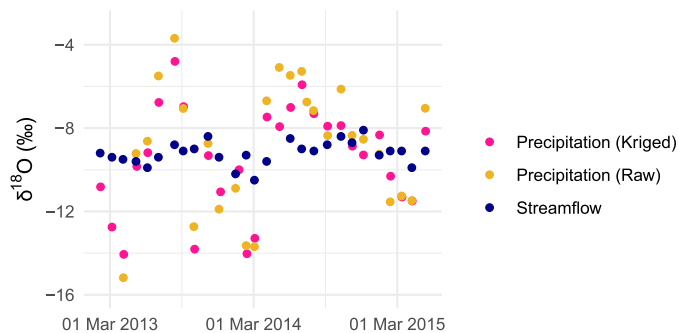


**Figure 2.** Data of  $\delta^{18}\text{O}$  in precipitation (kriged values as pink dots and raw values as yellow dots) and streamflow (blue dots).

### 3 Methods

#### 3.1 Catchment-scale transport model

In this study, we used the *tran-SAS* model (Benettin and Bertuzzo, 2018) for describing the catchment-scale water mixing and solute transport based on SAS functions. The catchment was conceptualized as a single storage  $S(t)$  (mm), whose water-age balance can be expressed as follows (Benettin and Bertuzzo, 2018):

$$S(t) = S_0 + V(t) \quad (1)$$

$$\frac{\partial S_T(T, t)}{\partial t} + \frac{\partial S_T(T, t)}{\partial T} = P(t) - Q(t) \cdot \Omega_Q(S_T, t) - ET(t) \cdot \Omega_{ET}(S_T, t) \quad (2)$$

110 Initial condition:  $S_T(T, t = 0) = S_{T0}(T)$  (3)

Boundary condition:  $S_T(0, t) = 0$  (4)

where  $S_0$  (mm) is the initial storage,  $V(t)$  (mm) are the storage variations,  $P(t)$  (mm/d),  $Q(t)$  (mm/d), and  $ET(t)$  (mm/d) are precipitation, discharge and evapotranspiration, respectively,  $S_T(T, t)$  (mm) is the age-ranked storage,  $S_{T0}(T)$  (mm) is the initial age-ranked storage, and  $\Omega_Q(S_T, t)$  (-) and  $\Omega_{ET}(S_T, t)$  (-) are the cumulative SAS functions for  $Q$  and  $ET$ , respectively.

115 By definition, the TTD of streamflow  $p_Q(T, t)$  ( $d^{-1}$ ) is calculated as follows (Benettin and Bertuzzo, 2018):

$$p_Q(T, t) = \frac{\partial \Omega_Q(S_T, t)}{\partial S_T} \cdot \frac{\partial S_T}{\partial T} \quad (5)$$

The isotopic signature in streamflow  $C_Q(t)$  (‰) can be obtained from (Benettin and Bertuzzo, 2018):

$$C_Q(t) = \int_0^{+\infty} C_S(T, t) \cdot p_Q(T, t) \cdot dT \quad (6)$$

where  $C_S(T, t)$  (‰) is the isotopic signature of a water parcel in storage. Equations 5 and 6 also apply for  $ET$ .

120 In this study, we tested three SAS parameterizations: the power law time-invariant (PLTI; Eq. 7 (Queloz et al., 2015)), power law time-variant (PLTV; Eq. 8 (Benettin et al., 2017)), and time-invariant beta (BETATI; Eq. 9 (Drever and Hrachowitz, 2017)) distribution. Here, they are expressed as probability density functions in terms of the normalized age-ranked storage  $P_S(T, t)$  (-), also known as fractional SAS functions (fSAS):

$$\omega(P_S(T, t), t) = k \cdot (P_S(T, t))^{k-1} \quad (7)$$

125  $\omega(P_S(T, t), t) = k(t) \cdot (P_S(T, t))^{k(t)-1}$  (8)

$$\omega(P_S(T, t), t) = \frac{(P_S(T, t))^{\alpha-1} \cdot (1 - P_S(T, t))^{\beta-1}}{B(\alpha, \beta)} \quad (9)$$

The parameters  $k$ ,  $\alpha$  and  $\beta$  determine the catchment's water age preference for outflows, while  $B(\alpha, \beta)$  is the two-parameter beta function. If  $k < 1$ , or if  $\alpha < 1$  and  $\beta > 1$ , the system tends to discharge young water. If  $k > 1$ , or if  $\alpha > 1$  and  $\beta < 1$ , the catchment

preferably releases old water. The case of  $k=1$  or  $\alpha=\beta=1$  describes no selection preference (i.e., complete water mixing). PLTV  
130 is characterized by  $k(t)$  varying linearly over time between two extremes  $k_1$  and  $k_2$  as a function of the catchment wetness  $w_i$  (-),  
i.e.,  $w_i(t) = (S(t)-S_{min})/(S_{max}-S_{min})$ , where  $S_{min}$  and  $S_{max}$  are the minimum and maximum storage values over the entire period.

### 3.2 Interpolation techniques for $\delta^{18}\text{O}$ in precipitation

We tested the model with two spatial representation and two temporal interpolation methods for  $\delta^{18}\text{O}_P$  to explore the impact  
of input tracer data on model performance, results, and uncertainty. To evaluate the effect of spatial representation, we firstly  
135 used single point  $\delta^{18}\text{O}_P$  measurement, which we refer to in the following as "raw"  $\delta^{18}\text{O}_P$ . These measurements, obtained from  
Lutz et al. (2018), were taken at the catchment outlet. The selection of  $\delta^{18}\text{O}_P$  at the outlet assumes a precipitation collector  
close to the stream gauge at the outlet, which is a common occurrence in many catchments for logistical reasons. Indeed, the  
outlet, where instream  $\delta^{18}\text{O}$  is sampled, serves as location where all precipitation inputs across the catchment are integrated.  
For convenience, precipitation monitoring is also often conducted at or near the gauging station at the outlet. Secondly, we used  
140 spatially interpolated  $\delta^{18}\text{O}_P$  with kriging based on multiple locations. The spatial interpolation was conducted in Lutz et al.  
(2018) using raw  $\delta^{18}\text{O}_P$  from 24 precipitation collectors spread over the larger Bode region, and altitude as external drift. In a  
further step, the kriged  $\delta^{18}\text{O}_P$  were weighted with spatially distributed monthly precipitation to obtain representative estimates  
for the study catchment. In our study, the kriged  $\delta^{18}\text{O}_P$  resulted in slightly more negative values than the raw  $\delta^{18}\text{O}_P$  from the  
catchment outlet (Fig. 2) because of the inclusion of more depleted  $\delta^{18}\text{O}_P$  values from locations with higher altitudes during  
145 the kriging process. By considering these two options for spatial representation of  $\delta^{18}\text{O}_P$ , we intend to assess the influence  
of spatial variability and uncertainty in the simulated outputs between two opposing cases i.e., raw isotopes representing the  
simplest approach and kriged isotopes derived from a more sophisticated method. While there are other possibilities for spatial  
representation of  $\delta^{18}\text{O}_P$ , our choice allows us to effectively address our research question regarding the effects on SAS models  
of tracer data in precipitation collected at a single location within the catchment or spatially interpolated from multiple sites.

150 SAS model results are sensitive to the choice of the temporal resolution of input tracer data, and a finer resolution is generally  
recommended to achieve a satisfactory level of detail (Benettin and Bertuzzo, 2018). Additionally, a forward Euler scheme was  
employed to solve Eq. 2, whose precision increases with high frequency time steps. For these reasons, we reconstructed daily  
 $\delta^{18}\text{O}_P$  estimates from monthly values with two interpolation schemes. First, we used a step function in which the values  
between two consecutive samples assumed the value of the last sample. Second, we used a sine interpolation due to the fact  
155 that  $\delta^{18}\text{O}_P$  samples typically exhibit pronounced seasonal variations with more depleted values in winter than in summer (Fig.  
2). The sine-wave function has been used in several studies to describe temporal variation in  $\delta^{18}\text{O}_P$  (McGuire and McDonnell,  
2006; Feng et al., 2009; Allen et al., 2019). The seasonal pattern of  $\delta^{18}\text{O}_P$  values over a period of one year can be described by  
(Kirchner, 2016):

$$\delta^{18}\text{O}_P(t) = a_P \cdot \cos(2 \cdot \pi \cdot f \cdot t) + b_P \cdot \sin(2 \cdot \pi \cdot f \cdot t) + k_P \quad (10)$$

160 where  $a$  and  $b$  are regression coefficients (-),  $t$  is the time (decimal years),  $f$  is the frequency ( $\text{yr}^{-1}$ ) and  $k$  is the vertical  
offset of the isotope signal (‰). The coefficients  $a$  and  $b$  were estimated by fitting Eq. 10 to monthly  $\delta^{18}\text{O}_P$  values using

the iteratively re-weighted least squares (IRLS) estimation (von Freyberg et al., 2018). In our study, we reproduced the daily frequency isotopic data through the estimated regression coefficients of Eq. 10. Figure 3 displays the daily kriged and raw  $\delta^{18}\text{O}_p$  values simulated via step function and sine interpolation; by employing step function and sine interpolation as techniques to reconstruct tracer data in precipitation, we aim to analyze the effects on SAS-based results from two relatively simple, rather opposing approaches: one focusing on individual measurements and the other on seasonality.

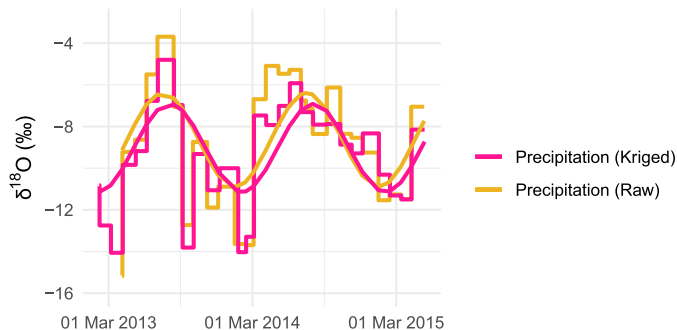


**Figure 3.** Predicted  $\delta^{18}\text{O}$  in precipitation (kriged values as pink lines and raw values as yellow lines) via step function and sine interpolation.

### 3.3 Experimental design

In this study, different scenarios were used to quantify uncertainty in the modeled results. We tested twelve setups composed of three SAS functions (PLTI, PLTV, BETATI), two temporal interpolation (step and sine function) and two spatial representations (raw and kriged values) of  $\delta^{18}\text{O}_p$  (Table 1). For each setup, we performed a Monte-Carlo experiment by running the model with 10,000 parameter sets generated by the Latin Hypercube Sampling (LHS; McKay et al., 1979). Model parameters and their search ranges are shown in Table 2. A 5 years warm-up period (i.e., repetition of the input data) from February 2008 to January 2013 was performed to reduce the impact of model initialization. The period from February 2013 to May 2015 was used to infer behavioral parameters (i.e., parameter sets giving acceptable predictions), and subsequently to interpret model results. The initial concentration of  $\delta^{18}\text{O}$  in storage was set to 9.2 ‰ coinciding with the mean  $\delta^{18}\text{O}_Q$  over the study period.

The informal likelihood of the Sequential Uncertainty Fitting Procedure (SUFI-2; Abbaspour et al., 2004) was applied to account for uncertainty in the parameter sets and resulting modeled estimates. In SUFI-2, the uncertainty is represented by a uniform distribution, which is gradually reduced until a specific criterion is reached. In our study, we calibrated the values of model parameters until the predicted output matched the measured  $\delta^{18}\text{O}_Q$  to a satisfactory level, defined by an objective function. We employed as objective function the Kling-Gupta efficiency (KGE; Gupta et al., 2009), and once the criterion of  $\text{KGE} \geq 0.5$  was satisfied, we defined a set of behavioral solutions for each model setup. However, since the aim of this study is to investigate the impact of various sources of uncertainty on simulated outputs rather than to determine the best model setup, we decided to set a fixed sample size and narrow down those solutions generated by SUFI-2 in the previous step. Setting a fixed sample size ensures comparability of results across the setups as different sample sizes could influence the uncertainty analysis i.e., the greater the number of behavioral solutions, the wider the uncertainty band. By fixing the sample size, we can still

**Table 1.** List of model setups.

setup	interpolation	SAS function
a	step function kriged $\delta^{18}\text{O}_P$	PLTI
b		PLTV
c		BETATI
d	step function raw $\delta^{18}\text{O}_P$	PLTI
e		PLTV
f		BETATI
g	sine function kriged $\delta^{18}\text{O}_P$	PLTI
h		PLTV
i		BETATI
j	sine function raw $\delta^{18}\text{O}_P$	PLTI
k		PLTV
l		BETATI

**Table 2.** Model parameters and search ranges.

SAS parameter	Symbol	Unit	Lower Bound	Upper Bound
Discharge SAS parameter	$k_Q$	[-]	0.1	2
	$k_{Q1}$	[-]	0.1	2
	$k_{Q2}$	[-]	0.1	2
	$\alpha$	[-]	0.1	2
	$\beta$	[-]	0.1	2
Evapotranspiration SAS parameter	$k_{ET}$	[-]	0.1	2
Initial storage	$S_0$	[mm]	300	3000

meet the requirement of a minimum acceptable KGE value (i.e.,  $\text{KGE} \geq 0.5$ ). In this study, we determined the final behavioral solutions by using a fixed sample size that corresponds to the best 5% parameter sets and modeled results in terms of KGE.

To assess the range of possible behavioral solution and understand the level of uncertainty associated with it, we calculated the 95% Confidence Interval (CI) derived by computing the 2.5% and 97.5% percentile values of the cumulative distribution in the parameters and time series of output variables (Abbaspour et al., 2004). These percentile values represent the lower and upper bounds of the CI, respectively. In our experimental setup, the main output variables were the instream  $\delta^{18}\text{O}$  signature and backward median transit time ( $\text{TT}_{50}$  (days), i.e., the time it takes for half of the water particles to leave the system as streamflow at the catchment outlet). Time series of  $\text{TT}_{50}$  were extracted directly from daily TTDs (Eq. 5) and used as a metric for the streamflow age. This was done because TTDs are typically skewed with long tails (Kirchner et al., 2001), hence the median is often a more suitable metric than, for example, MTT as it is less impacted by the poor identifiability of the older water components (Benettin et al., 2017).



## 4 Results

### 4.1 Simulated $\delta^{18}\text{O}$ in streamflow and model performances

modeled  $\delta^{18}\text{O}$  in streamflow ( $\delta^{18}\text{O}_Q$ ) represented by the 95% confidence interval (CI) in the ensemble solution are displayed in Fig. 4. The results reveal how the predicted  $\delta^{18}\text{O}_Q$  values enveloped the measured isotopic signature by reproducing its seasonal fluctuations, with depleted (i.e., more negative) values in winter and enriched (i.e., less negative) values in summer. Although the behavioral parameter sets were able to capture the seasonal isotopic trend, they poorly reproduced the exact values; therefore, the ensemble simulations are characterized by a non-negligible uncertainty.

Figure 4 shows the distinct effects of the interpolated input tracer data and model parameterization on the simulated  $\delta^{18}\text{O}_Q$  values. The step function interpolation generated an erratic isotopic signature in streamflow with flashy fluctuations (Fig. 4a-f). On the other hand, sine interpolation of  $\delta^{18}\text{O}_P$  values yielded a smooth response in the simulated  $\delta^{18}\text{O}_Q$  values (Fig. 4g-l). No significant visual distinction was found between kriged (Fig. 4a-c) and raw (Fig. 4d-f)  $\delta^{18}\text{O}_P$  samples when the step function interpolation is used, except for a slightly larger uncertainty observed with raw  $\delta^{18}\text{O}_P$  samples. Furthermore, when employing the sine interpolation and raw  $\delta^{18}\text{O}_P$  values (Fig. 4j-l) the simulations overestimated the instream measurements in comparison to kriged values (Fig. 4g-i). Finally, distinct SAS parameterizations did not produce remarkable differences in the simulated  $\delta^{18}\text{O}_Q$  values, although PLTV generally yielded simulations that better enveloped the measured isotopic signature (Fig. 4b, e, h and k).

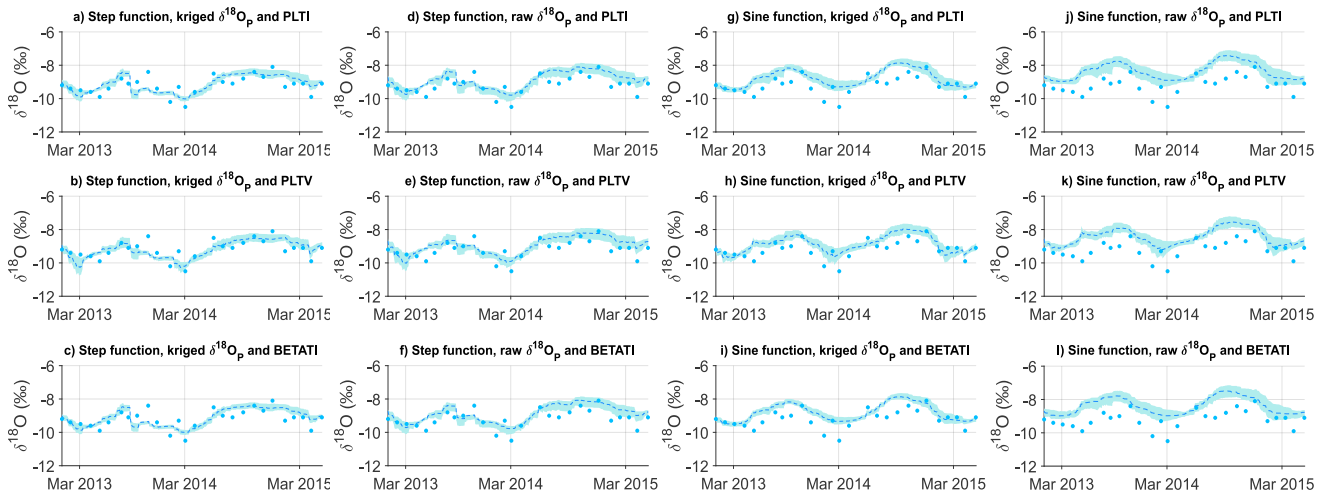


**Figure 4.** Predicted  $\delta^{18}\text{O}$  values in streamflow. Dark blue filled circles represent the observed data; the light blue line and the shaded area represent, respectively, the ensemble mean of all possible solutions and their range according to the 95% CI.

Despite the differences in the predicted  $\delta^{18}\text{O}_Q$  values, all simulations can be considered satisfactory given the KGE values ranging between 0.55 and 0.72, across all tested setups (Fig. 5). These performances can be classified from intermediate (Thiemig et al., 2013) to good (Andersson et al., 2017; Sutanudjaja et al., 2018). When considering the best fit, the combi-

nation of the step function interpolation and raw  $\delta^{18}\text{O}_p$  values performed best. Additionally, PLTV generally yielded slightly better KGE values than PLTI and BETATI when grouping the setups with the same spatio-temporal interpolation of  $\delta^{18}\text{O}_p$ . Differences in the mean KGEs were statistically insignificant (t-test with p-values  $> 0.05$ ) only between setups c and i, and c and k (Table 1) as the mean KGE values were nearly identical; this largely agrees with the visual analysis (Fig. 5). Contrarily, the differences in the mean KGE values of the remaining setups were statistically significant (p-values  $< 0.05$ ), indicating that a priori methodological choice (i.e., interpolation techniques of  $\delta^{18}\text{O}_p$  values and/or SAS parameterization) strongly impact on the overall results. Nonetheless, this does not mean that we can clearly identify the most suitable setup, but there is need to carefully analyze the multiple potential choices in SAS parameterization and tracer data interpolations, and to evaluate the uncertainty range in modeled predictions.

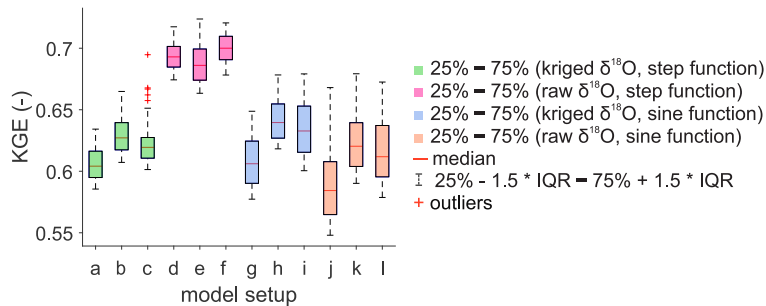


**Figure 5.** Boxplot of model performance ranges in behavioral solutions. The letters on the x-axis refer to the model setup type according to Table 1. Boxplots filled with the same colors represent model setups characterized by the same interpolation scheme in space and time. On each box, the central red line indicates the median, and the bottom and top edges of the box indicate the 25th and 75th percentiles respectively, namely the interquartile range (IQR). The whiskers extend to the most extreme data points not considered outliers which are 25th percentile minus 1.5 times IQR and 25th percentile plus 1.5 times IQR, respectively. The outliers are plotted individually using the red '+' mark.

Ranges of the behavioral SAS parameters for the tested setups are summarized in Table S1 in the Supplement. Parameters for the SAS functions of  $Q$  (i.e.,  $k_Q$ ,  $k_{Q1}$ ,  $k_{Q2}$ ,  $\alpha$  and  $\beta$ ) were different across the setups although, in general, they were relatively narrow and well identified. However, the behavioral parameters were better constrained when using the step function interpolation since their 95% CI was, on average, 34% narrower than that provided by the sine interpolation, across all the SAS parameterizations. The parameters  $k_{Q1}$  and  $\alpha$  were also better identified than  $k_{Q2}$  and  $\beta$ , since their 95% CI was, on average, 56% narrower, across all tested setups. Conversely, there was no clear difference in the parameters ranges when using kriged or raw  $\delta^{18}\text{O}_p$  values. The evapotranspiration parameter (i.e.,  $k_{ET}$ ) was poorly identified in all setups as any value in the search range provided equally good results. The initial storage (i.e.,  $S_0$ ) was only partially constrained as any value between 335 mm and 2895 mm was considered acceptable.

## 4.2 Simulated transit times and model uncertainty

Figure 6 illustrates the 95% CI of the behavioral solutions for the predicted median transit time ( $\text{TT}_{50}$ ). The results show that the model simulated largely different ranges of  $\text{TT}_{50}$  based on the tested setups. When using PLTI and BETATI (Fig. 6a, c, d,

f, g, i, j and l), the 95% CI was relatively stable with smaller fluctuations throughout the simulation period, compared to PLTV (Fig. 6b, e, h and k). However, minor differences emerged across the simulated  $TT_{50}$  as a result of the distinct interpolation techniques used for  $\delta^{18}O_P$ . The 95% CI of  $TT_{50}$  was on average larger by 37%, across all tested setups, when using raw  $\delta^{18}O_P$  (Fig. 6d-f and j-l) rather than kriged  $\delta^{18}O_P$  (Fig. 6a-c and g-i). This was especially visible when the step function was used (Fig. 6a-f). Moreover, the sine interpolation generated a 95% CI of  $TT_{50}$  being on average 62% narrower across all tested setups (Fig. 6g-l) with respect to the step function (Fig. 6a-f). These differences were more evident for high flow conditions where the 95% CI of  $TT_{50}$  showed a significant reduction. In addition, the behavioral solutions obtained with the sine interpolation (Fig. 6g-l) were more skewed towards shorter mean  $TT_{50}$  values, across all tested setups, than those of the step function (Fig. 6a-f).

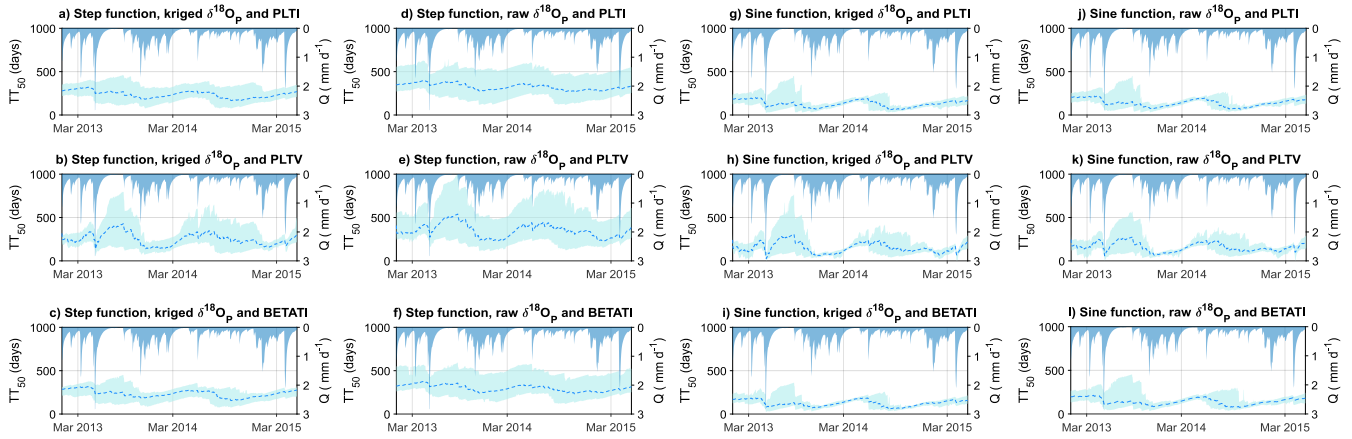


**Figure 6.** Predicted  $TT_{50}$  of streamflow; the light blue line and the shaded area represent, respectively, the ensemble mean of all possible solutions and their range according to the 95% CI.

Behavioral solutions obtained with PLTV revealed a similar pattern regardless of the interpolation employed (Fig. 6b, e, h and k). Nonetheless, there was a noticeable difference in the 95% CI of  $TT_{50}$  under distinct flow regimes. During low flows and dry periods (i.e., summer and autumn), the time series of predicted  $TT_{50}$  showed large uncertainties ranging at most between 259 and 1009 days across the different setups (Fig. 6e). Conversely, during high flows (i.e., winter and spring), the 95% CI was much narrower and varied at least between 126 and 154 days (Fig. 6h). The large 95% CI and the notable differences across the tested setups highlight the sensitivity and, in turn, the uncertainty of predicted  $TT_{50}$  to the model parameterization, temporal interpolation of input data, hydrologic conditions and non-spatially interpolated  $\delta^{18}O_P$ .

In general, the variability of the predicted  $TT_{50}$  was controlled by the hydrological state of the system (Fig. 6). High discharge events reduced the  $TT_{50}$  values, while low flow periods were associated with a longer estimated  $TT_{50}$ . This is expected as streamflow during high (low) flows is dominated by near-surface runoff (groundwater) with shallow (deep) flowpaths leading to a shorter (longer)  $TT_{50}$ . Such differences were particularly visible with PLTV (Fig. 6b, e, h, and k) as the exponent  $k_Q(t)$  shift the water selection preference over time as a function of the wet/dry conditions. This resulted in the variability of  $TT_{50}$  being more pronounced than that of PLTI and BETATI, whose SAS parameters for  $Q$  are constant over time.

### 4.3 Catchment-scale water release

SAS functions provided valuable insights into the catchment-scale water release dynamics. Figure 7 presents the behavioral solutions releasing water of different ages, and shows that the catchment generally experienced a stronger affinity for realising young water (i.e.,  $k_Q < 1$ , or  $\alpha < 1$  and  $\beta > 1$ ), rather than old water (i.e.,  $k_Q > 1$ , or  $\alpha > 1$  and  $\beta < 1$ ). These findings are in agreement with other studies in the Upper Selke (Winter et al., 2020; Nguyen et al., 2021). Nonetheless, there were differences in the water release scheme when comparing various combinations of SAS functions and spatio-temporal interpolation techniques of isotopes. The use of PLTV resulted in a substantial number of solutions, approximately 50% of all behavioral solutions, suggesting a preference for both young and old water. On the other hand, only a few solutions showed affinity for old water release, and this was more prominent when using the sine interpolation, raw  $\delta^{18}\text{O}_p$  values and PLTI across all tested setups.

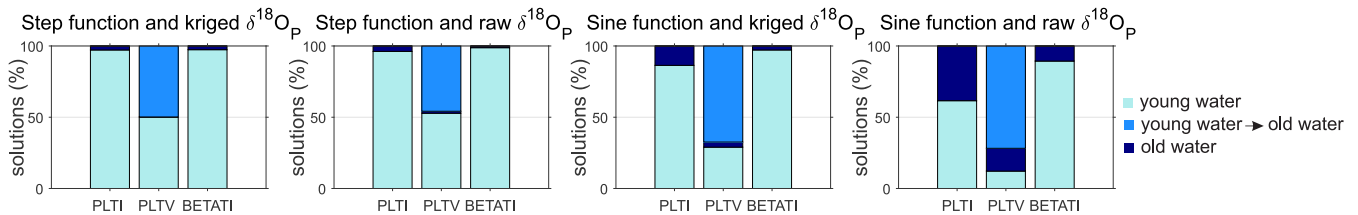


**Figure 7.** Percentage of behavioral solutions releasing water of different ages.

## 5 Discussion

### 5.1 Uncertainty in TTD modelling

In this study, we characterized the TTD uncertainty arising from some significant and critical aspects for the SAS modelling. These aspects are also the most directly linked to data interpolation and SAS parameterization that we explored in this work. The uncertainty analysis was carried out across the twelve tested setups corresponding to different combinations of spatio-temporal data interpolation techniques and SAS parameterizations. Our results show that the uncertainty (i.e., 95% CI) of the simulated  $\text{TT}_{50}$  (Fig. 6) was firmly dependent on the choice of model setup, as the 95% CI was primarily sensitive to the type of SAS function, temporal interpolation and spatial representation of  $\delta^{18}\text{O}_p$ .

Uncertainty in the simulated  $\text{TT}_{50}$  differed considerably between time-invariant (i.e. PLTI and BETATI; Fig. 6a, c, d, f, g, i, j and l) and time-variant (i.e., PLTV; Fig. 6b, e, h and k) SAS functions, thus a large sensitivity is associated with the choice of the SAS parameterization. For example, PLTI and BETATI explicitly assume constant water selection preference over time as these functions do not consider temporal variability of the catchment wetness. As a consequence, the resulting  $\text{TT}_{50}$  had a moderately stable 95% CI with smaller fluctuations compared to those of PLTV. On the other hand, including an explicit time dependence in the SAS function strongly affected the 95% CI of  $\text{TT}_{50}$ . PLTV produced a wider 95% CI notably during low flow conditions, which can hinder the TTDs ability to provide robust insights on flow and solute transport behaviors in the study area during low flow conditions. This highlights the need to further constrain PLTV with additional data, which could involve

obtaining tracer data at a finer resolution or additional information on the evapotranspiration and initial storage. In addition, the exceptionally old flow components associated with a very large 95% CI of  $TT_{50}$  might be a distortion of the actual  $TT_{50}$  values, which can usually be more reliably estimated using radioactive tracers rather than stable isotopes (Visser et al., 2019). Hence, PLTV-based  $TT_{50}$  greater than the observed period (828 days) should be interpreted carefully. It is important to note that in this study we discussed the fractional (fSAS) functions, while another form of the SAS functions, such as the rank SAS (rSAS) functions, may have different uncertainty. This is mainly due to the difference in how the storage is considered, because fSAS functions are expressed as function of the normalized age-ranked storage, which is equal to the cumulative residence time, while rSAS functions depend on the age-ranked storage, which is the volume of water in storage ranked from youngest to oldest (Harman, 2015).

Likewise, the high-frequency reconstruction of  $\delta^{18}O_P$  from monthly samples via interpolation created further uncertainty. The sine interpolation effectively captured the dominant features of the observed  $\delta^{18}O_P$ , such as seasonality. Consequently, sine interpolation successfully reproduced the seasonal trend in instream  $\delta^{18}O$ , although simulations overestimated the measurements (Fig. 4g-l). On the other hand, sine interpolation poorly reproduced rainfall isotopes during short-term flashy events and missed detailed characteristics of the tracer dataset by smoothing the variability in the observed  $\delta^{18}O_P$  (Fig. 3). As a result, high values of  $\delta^{18}O_P$  are underestimated, whereas low values are overestimated. It is critical to recognize these limitations when interpreting modelling results as uncertainty in the simulated  $\delta^{18}O_P$  may conceal a more pronounced hydrological response of the system (Dunn et al., 2008; Birkel et al., 2010; Hrachowitz et al., 2011). Contrarily, step function interpolation preserved the maxima in the monthly observed  $\delta^{18}O_P$  values by capturing their variation correctly (Fig. 3). Simulations showed a better fit with measured instream  $\delta^{18}O$  (Fig. 4a-f) and higher model performance (Fig. 5). However, combining step function with raw  $\delta^{18}O_P$  resulted in larger uncertainty of simulated  $TT_{50}$  (Fig. 6d-f). This reflects the need for a comprehensive exploration of the uncertainty range, rather than relying solely on the goodness-of-fit. Overall, the choice between step function and sine interpolation largely affected the reconstructed input data (Fig. 3), leading to significant differences in simulated  $TT_{50}$  and associated uncertainty. It is important to note that alternative methods, such as Generalized Additive Models (GAM; Buzacott et al., 2020), offer other options for interpolating tracer data. We conducted further tests with the SAS model using GAM to reconstruct both kriged and raw  $\delta^{18}O_P$  using smoothing functions; this provides a more sophisticated approach than the intuitive methods used in this study. However, the results, available in the Supplement, show that while GAM provided more detailed reconstructed input tracer data (Fig. S1), it did not significantly alter the SAS-based results (Figs. S2 and S3) or yield any new insights or conclusions about uncertainty with respect to using step function and sine interpolation. Therefore, we conclude that while highly resolved input data may seem appealing, it does not necessarily lead to substantial benefits for the SAS-based output, supposedly due to the conceptual simplifications in the SAS model.

The spatial representation of  $\delta^{18}O_P$  values had limited impact on the overall pattern of simulated  $TT_{50}$  as the time series were comparable with both kriged (Fig. 6a-c and g-i) and raw (Fig. 6d-f and j-l)  $\delta^{18}O_P$ . Nonetheless, the spatial interpolation of  $\delta^{18}O_P$  from different locations resulted in a reduction in the uncertainty of  $TT_{50}$ , which was particularly evident with step function (Fig. 6a-f). This difference may be attributed to the fact that the Upper Selke is a large (mesoscale) catchment with a substantial gradient in elevation, and, as a consequence, measurement for  $\delta^{18}O_P$  from only one location may be generally

overly simplistic. This finding highlights the importance of considering not only the model performance (Fig. 5; raw values with a step function interpolation produced higher KGE values), but also the uncertainty range in predicted  $TT_{50}$ .

320 Finally, we found that the uncertainty was larger under dry conditions when lower flow and longer  $TT_{50}$  were observed. This was especially visible when using the time-variant SAS function (Fig. 6b, e, h and k). It might be due to the fact that under wet conditions, there is a high level of hydrologic connectivity within the catchment (Ambroise, 2004; Blume and van Meerveld, 2015; Hrachowitz et al., 2016), which results in nearly all flow paths being active and contributing to the streamflow. This, ultimately, may make  $TT_{50}$  values easier to constrain. Conversely, under dry conditions, when usually only longer flowpaths  
325 carrying older water are active (Soulsby and Tetzlaff, 2008; Jasechko et al., 2017), water partially flows through a drier soil zone where flow is more erratic (i.e. flow directions and patterns can vary widely) as the conductivity is controlled by soil moisture. As a result, wet areas can be patchy and water flows preferentially at certain locations only, as opposed to spatially uniform flow through the soil matrix; this might make it more challenging to constrain older water ages. Similarly, Benettin et al. (2017) found higher uncertainty in the simulated SAS-based median water ages during drier periods, potentially due to  
330 higher uncertainty in the total storage. Moreover, non-SAS functions studies have observed major uncertainties and deviations from observations in lumped modeled results during low flow conditions (Kumar et al., 2010). This was primarily due to the lack of spatial variability of catchment characteristics in lumped models, a critical factor controlling low flow regimes in rivers.

The dissimilarities in the simulated  $TT_{50}$  across the tested setups underline the importance of accounting for uncertainty in model-based TTDs. The uncertainty analysis with SUFI-2 performed in this study was essential to best describe the parameter  
335 identifiability and bounds of the behavioral solutions of each output variable. Furthermore, our results highlight the importance of gaining tracer datasets of good quality (i.e., tracer data with a finer temporal resolution), considering the spatial variability of the isotopic composition in precipitation and, possibly, employing a model parameterization that best describes the catchment-specific storage and release dynamics. The last point can be defined according to a precise conceptual knowledge of the catchment's functioning and information from previous studies in similar catchments.

## 340 **5.2 TTD modelling: advantages and limitations**

Our results provide visually plausible seasonal fluctuations of the predicted  $\delta^{18}O_Q$  samples (Fig. 4), and satisfactory KGE values (Fig. 5), despite the uncertainty arising from model inputs, structure and parameters. The good match with observations provides confidence in the simulated  $TT_{50}$  for the Upper Selke. The magnitude of the uncertainty resulting from different setups cannot be generalized, but the overall approach for uncertainty assessment presented here could be extended to other areas and  
345 TTD studies. However, we recognize some limitations and indicate below possible reasons and, in turn, improvements that future work could achieve.

First, the limited length of the  $\delta^{18}O$  time series might not describe the system accurately, hence implementing longer time series could improve the parameter identifiability and provide a more accurate estimation of the TTDs. Second, this study relied on stable water isotopes, which might underestimate the tails of the TTDs (Stewart et al., 2010; Seeger and Weiler, 2014; Wang  
350 et al., 2022). Possible advancements could be reached by using decaying tracers varying over a larger timescale than stable water isotopes (e.g., tritium; Stewart et al., 2012; Morgenstern et al., 2015), and imparting more information on old water.

Next, future work should retrieve more information on the evapotranspiration  $ET$  and initial storage  $S_0$ , whose parameters were poorly identified. However, this issue is common in transport studies that rely on measurements of instream stable water isotopes (Benettin et al., 2017; Buzacott et al., 2020). As a way forward, information on the  $ET$  isotopic compositions might help better constrain  $ET$  parameters and assess their affinity for young/old water. Regarding constraining the range of  $S_0$ , further information can be gained from geophysical surveys in the study areas or groundwater modelling, as well as using decaying isotopes (Visser et al., 2019).

### 5.3 Implications of TTD uncertainties

This study characterized the uncertainty in TTDs, which summarize the catchment's hydrologic transport behavior, and thereby comprise decisive information for water managers. The value of  $TT_{50}$  has relevant implications for both water quantity and quality, as does its uncertainty. The larger the 95% CI in the simulated  $TT_{50}$ , the greater the difference in the  $TT_{50}$  values, which, ultimately, implies distinct hydrological processes, water availability, groundwater recharge and solute export dynamics (McDonnell et al., 2010).

For example, knowing the TTD and its uncertainty may be crucial for characterizing the catchment's response to climatic change (Wilusz et al., 2017). Considering the increasing severity of droughts in the past decades (Dai, 2013), a catchment with a shorter  $TT_{50}$  and a dominant release of young water might be more affected by droughts than a catchment with a longer  $TT_{50}$ , which means that its stream is fed by relatively old water sources. Therefore, a short  $TT_{50}$  reveals a low drought resilience of the catchment and limited water availability, which could limit streamflow generation processes and change the instream water quality status during drought periods (Winter et al., 2023). Likewise, TTD uncertainty may affect the understanding of the water infiltration rate, hydrological processes and aquifer recharge, as a shorter  $TT_{50}$  suggests that water is quickly routed to the catchment outlet rather than infiltrating deeply into the groundwater. Finally, TTD uncertainty can have an impact on the quantification of the modern groundwater age, i.e., groundwater younger than 50 years (Bethke and Johnson, 2008). According to Jasechko (2019), the correct identification of modern groundwater abundance and distribution can help determine its renewal (Le Gal La Salle et al., 2001; Huang et al., 2017), groundwater wells and depths most likely to contain contaminants (Visser et al., 2013; Opazo et al., 2016), and the part of the aquifer flushed more rapidly.

Uncertainty in TTDs also impacts on assessing the fate of dissolved solutes, such as nitrates (Yang, X. et al., 2018; Nguyen et al., 2021, 2022; Lutz et al., 2022), pesticides (Holvoet et al., 2007; Lutz et al., 2017), and chlorides (Kirchner et al., 2000; Benettin et al., 2013). These solutes constitute a crucial source of diffuse water pollution in agricultural areas (Jiang et al., 2014; Kumar et al., 2020), as they are spread on the soil in large quantities especially during the growing season. Exposure time of solutes with the soil matrix has strong consequences for biogeochemical reactions, such as denitrification in the case of nitrates (Kolbe et al., 2019; Kumar et al., 2020). A short  $TT_{50}$  suggests that water can be rapidly conveyed to the stream network (Kirchner et al., 2001), with limited time for denitrification. This explains the elevated instream concentration and short-term impact of nitrate export compared to that of a longer  $TT_{50}$ , which is typically associated with old water release and low nitrate concentration (Nguyen et al., 2021). Similarly, pesticide transport is highly affected by the TTD uncertainty as a long  $TT_{50}$  suggests little pesticide degradation due to decreased microbial activity along deeper flowpaths (Rodríguez-Cruz

et al., 2006). In other cases, a shorter  $TT_{50}$  may limit the time for degradation causing a peak in the instream concentration (Leu et al., 2004). Overall, a longer  $TT_{50}$  can delay or buffer the catchment's reactive solute response at the outlet (Dupas et al., 2016; Van Meter et al., 2017). This creates a long-term effect of hydrological legacies and a continuous problem with diffuse pollution of nitrates (Ehrhardt et al., 2019; Winter et al., 2020) and pesticides (Lutz et al., 2013), which can persist in the catchment for several years. Finally, TTD uncertainties also play an important role in chloride transport, although chlorides are commonly known to be conservative (Svensson et al., 2012). A short  $TT_{50}$  may indicate rapid chloride mobilization, whereas a long  $TT_{50}$  implies chloride persistence in groundwater; thereby chloride accumulates and is released at lower rates, with impacts on the ecosystem functions, vegetation uptake and metabolism (Xu et al., 1999).

Understanding the uncertainty in TTDs is crucial for the aforementioned implications. While previous studies have used only a specific SAS function and/or specific tracer data interpolation technique in time and space, here we show that there could be a wide range of different results in terms of water ages, model performances and parameter uncertainty. This is due to the specific choice regarding SAS parameterization and tracer data interpolation. With this, we want to convey that uncertainty is omnipresent in TTD-based models, and we need to recognise it, especially when dealing with sparse tracer data and multiple choices for model parameterization. Therefore, we want to encourage future studies to explore these uncertainties in other catchments and different geophysical settings, with the final aim to investigate whether these uncertainties may affect the conclusions of water quantity and quality studies for management purposes.

## 6 Conclusions

This study explored the uncertainty in TTDs of streamflow, resulting from twelve model setups obtained from different SAS parameterizations (i.e., PLTI, PLTV and BETATI), and reconstruction of the precipitation isotopic signature in time and space via interpolation (step function vs. sine-fit, raw vs. kriged values).

We found satisfactory KGE values, whose differences across the tested setups were statistically significant, meaning that the choice of the setup matters. As a consequence, distinct setups led to considerably different simulated  $TT_{50}$  values. The choice between using time-variant or time-invariant SAS functions was crucial as the time-invariant functions generated moderate fluctuations in the 95% CI of the estimated  $TT_{50}$  because of the constant water selection preference over time. On the other hand, the time-variant SAS function captured the dynamics of the catchment wetness, resulting in more pronounced fluctuations of  $TT_{50}$ . However, the time-variant SAS function also produced a larger 95% CI in  $TT_{50}$ , notably during drier periods, which might indicate the need to constrain the function with additional data (e.g., finer tracer data resolution, and/or information on evapotranspiration and storage). Significant differences in  $TT_{50}$  were observed depending on the employed temporal interpolations. Results from the sine interpolation produced a smaller uncertainty in  $TT_{50}$ , with the time series skewed towards smaller values. However, such results must be interpreted carefully as the sine interpolation poorly reproduced flashy events in precipitation, thus indicating that some more dynamic transport processes were not fully accounted for. Conversely, the step function interpolation resulted in a larger uncertainty of  $TT_{50}$ , but it was able to better reproduce the measured  $\delta^{18}O_p$  data by capturing the peak values, as opposed to the sine interpolation. Dry conditions were another reason for uncertainty as indicated



by the high variance in the simulated  $TT_{50}$  values, which is potentially attributed to the water preferentially moving at certain  
420 locations, making wet areas patchy, so it may be more challenging to accurately constrain older water ages. Finally, there  
was comparable pattern in the modeled results when using kriged versus raw isotopes, but the kriged values yielded an un-  
certainty reduction in  $TT_{50}$ . This highlights the potential advantage of spatially interpolated values over a single measurement  
representative of the entire area, particularly in mesoscale catchment varying in elevation.

These findings provide new insights into TTD uncertainty when high-frequency tracer data are missing and the SAS frame-  
425 work is used. Regardless of the degree of efficiency or uncertainty, the decision on which setup is more plausible depends on  
the best conceptual knowledge of the catchment functioning. We consider the presented approach as potentially applicable to  
other studies for enabling a better characterization of TTDs uncertainty, improving TTD simulations and, ultimately, informing  
water management. These aspects are particularly crucial in view of evermore extreme climatic conditions and increasing water  
pollution under global change.

430 *Code and data availability.* The model used in this study is presented at <https://doi.org/10.5194/gmd-11-1627-2018>. The iteratively re-  
weighted least squares (IRLS) method used to get modeled daily kriged and raw isotope ( $\delta^{18}O$ ) in precipitation with the sine interpolation  
is presented at <https://doi.org/10.5194/hess-22-3841-2018>. Hydroclimatic time series,  $\delta^{18}O$  data and interpolated  $\delta^{18}O$  time series can be  
accessed at <https://doi.org/10.5281/zenodo.6630477>.

*Author contributions.* AB conducted the model simulations, the analysis and interpretation of the results, and wrote the original draft of the  
435 paper. SRL and RK designed and conceptualized the study, and provided data for model simulations. TVN provided technical support for  
modelling and helped organize the structure and content of the paper. AB, SRL, RK and TVN conceived the methodology and experimental  
design. All co-authors helped AB interpret the results. All authors contributed to the review, final writing and finalization of this work.

*Competing interests.* RK is a member of the editorial board of Hydrology and Earth System Sciences.

## References

- 440 Abbaspour, K. C., Johnson, C. A., and van Genuchten, M. T.: Estimating uncertain flow and transport parameters using a sequential uncertainty fitting procedure, *Vadose Zone Journal*, 3(4), 1340–1352, <https://doi.org/10.2136/vzj2004.1340>, 2004.
- Ajami, N. K., Duan, Q., and Sorooshian, S.: An integrated hydrologic Bayesian multimodel combination framework: Confronting input, parameter, and model structural uncertainty in hydrologic prediction, *Water Resour. Res.*, 43, W01403, <https://doi.org/10.1029/2005WR004745>, 2007.
- 445 Allen, S. T., Jasechko, S., Berghuijs, W. R., Welker, J. M., Goldsmith, G. R., and Kirchner, J. W.: Global sinusoidal seasonality in precipitation isotopes, *Hydrol. Earth Syst. Sci.*, 23, 3423–3436, <https://doi.org/10.5194/hess-23-3423-2019>, 2019.
- Ambroise, B.: Variable 'active' versus 'contributing' areas or periods: a necessary distinction, *Hydrol. Process.*, 18, 1149–1155, <https://doi.org/10.1002/hyp.5536>, 2004.
- Andersson, J. C. M., Arheimer, B., Traoré, F., Gustafsson, D., , and Ali, A.: Process refinements improve a hydrological model concept  
450 applied to the Niger River basin, *Hydrol. Process.*, 31, 4540–4554, <https://doi.org/10.1002/hyp.11376>, 2017.
- Asadollahi, M., Stumpp, C., Rinaldo, A., and Benettin, P.: Transport and water age dynamics in soils: A comparative study of spatially integrated and spatially explicit models, *Water Resour. Res.*, 56, e2019WR025539, <https://doi.org/10.1029/2019WR025539>, 2020.
- Benettin, P. and Bertuzzo, E.: tran-SAS v1.0: a numerical model to compute catchment-scale hydrologic transport using StorAge Selection functions, *Geosci. Model Dev.*, 11, 1627–1639, <https://doi.org/10.5194/gmd-11-1627-2018>, 2018.
- 455 Benettin, P., van der Velde, Y., van der Zee, S. E. A. T. M., Rinaldo, A., and Botter, G.: Chloride circulation in a lowland catchment and the formulation of transport by travel time distributions, *Water Resour. Res.*, 49, 4619–4632, <https://doi.org/10.1002/wrcr.20309>, 2013.
- Benettin, P., Bailey, S. W., Campbell, J. L., Green, M. B., Rinaldo, A., Likens, G. E., J., M. K., and Botter, G.: Linking water age and solute dynamics in streamflow at the Hubbard Brook Experimental Forest, NH, USA, *Water Resour. Res.*, 51, 9256–9272, <https://doi.org/10.1002/2015WR017552>, 2015a.
- 460 Benettin, P., Kirchner, J. W., Rinaldo, A., and Botter, G.: Modeling chloride transport using travel time distributions at Plynlimon, Wales, *Water Resour. Res.*, 51, 3259–3276, <https://doi.org/10.1002/2014WR016600>, 2015b.
- Benettin, P., Soulsby, C., Birkel, C., Tetzlaff, D., Botter, G., and Rinaldo, A.: Using SAS functions and high-resolution isotope data to unravel travel time distributions in headwater catchments, *Water Resour. Res.*, 53, 1864–1878, <https://doi.org/10.1002/2016WR020117>, 2017.
- Bethke, C. M. and Johnson, T. M.: Groundwater age and groundwater age dating, *Annu. Rev. Earth Planet. Sci.*, 36, 121–152,  
465 <https://doi.org/10.1146/annurev.earth.36.031207.124210>, 2008.
- Beven, K.: A manifesto for the equifinality thesis, *J. Hydrol.*, 320, 18–36, <https://doi.org/10.1016/j.jhydrol.2005.07.007>, 2006.
- Beven, K. and Freer, J.: Equifinality, data assimilation, and uncertainty estimation in mechanistic modelling of complex environmental systems using the GLUE methodology, *J. Hydrol.*, 249, 11–29, [https://doi.org/10.1016/S0022-1694\(01\)00421-8](https://doi.org/10.1016/S0022-1694(01)00421-8), 2001.
- Birkel, C. and Soulsby, C.: Advancing tracer-aided rainfall-runoff modelling: A review of progress, problems and unrealised potential,  
470 *Hydrol. Process.*, 29, 5227–5240, <https://doi.org/10.1002/hyp.10594>, 2015.
- Birkel, C., Dunn, S. M., Tetzlaff, D., and Soulsby, C.: Assessing the value of high-resolution isotope tracer data in the stepwise development of a lumped conceptual rainfall-runoff model, *Hydrol. Process.*, 24, 2335–2348, <https://doi.org/10.1002/hyp.7763>, 2010.
- Blume, T. and van Meerveld, H. J.: From hillslope to stream: methods to investigate subsurface connectivity, *WIREs Water*, 2, 177–198, <https://doi.org/10.1002/wat2.1071>, 2015.

- 475 Botter, G., Bertuzzo, E., Bellin, A., and Rinaldo, A.: On the Lagrangian formulations of reactive solute transport in the hydrologic response, *Water Resour. Res.*, 41, W04008, <https://doi.org/10.1029/2004WR003544>, 2005.
- Botter, G., Bertuzzo, E., and Rinaldo, A.: Transport in the hydrologic response: Travel time distributions, soil moisture dynamics, and the old water paradox, *Water Resour. Res.*, 46, W03514, <https://doi.org/10.1029/2009WR008371>, 2010.
- Botter, G., Bertuzzo, E., and Rinaldo, A.: Catchment residence and travel time distributions: The master equation, *Geophys. Res. Lett.*, 38, L11403, <https://doi.org/10.1029/2011GL047666>, 2011.
- 480 Buzacott, A. J. V., van der Velde, Y., Keitel, C., and Vervoort, R. W.: Constraining water age dynamics in a south-eastern Australian catchment using an age-ranked storage and stable isotope approach, *Hydrol. Process.*, 34, 4384–4403, <https://doi.org/10.1002/hyp.13880>, 2020.
- Dai, A.: Erratum: Increasing drought under global warming in observations and models, *Nature Clim Change*, 3, 171, <https://doi.org/10.1038/nclimate1811>, 2013.
- 485 Danesh-Yazdi, M., Fofoula-Georgiou, E., Karwan, D. L., and Botter, G.: Inferring changes in water cycle dynamics of intensively managed landscapes via the theory of time-variant travel time distributions, *Water Resour. Res.*, 52, 7593–7614, <https://doi.org/10.1002/2016WR019091>, 2016.
- Danesh-Yazdi, M., Klaus, J., Condon, L. E., and Maxwell, R. M.: Bridging the gap between numerical solutions of travel time distributions and analytical storage selection functions, *Hydrol. Process.*, 32, 1063–1076, <https://doi.org/10.1002/hyp.11481>, 2018.
- 490 Yang, J., Heidbüchel, I., Musolff, A., Reinstorf, F., and Fleckenstein, J. H.: Exploring the Dynamics of Transit Times and Subsurface Mixing in a Small Agricultural Catchment, *Water Resour. Res.*, 54, 2317–2335, <https://doi.org/10.1002/2017WR021896>, 2018.
- Yang, X., Seifeddine, J., Zink, M., Fleckenstein, J. H., Borchardt, D., and Rode, M.: A New Fully Distributed Model of Nitrate Transport and Removal at Catchment Scale, *Water Resour. Res.*, 54, 5856–5877, <https://doi.org/10.1029/2017WR022380>, 2018.
- Drever, M. C. and Hrachowitz, M.: Migration as flow: using hydrological concepts to estimate the residence time of migrating birds from the daily counts, *Methods Ecol. Evol.*, 8, 1146–1157, <https://doi.org/10.1111/2041-210X.12727>, 2017.
- 495 Dunn, S. M., Bacon, J. R., Soulsby, C., Tetzlaff, D., Stutter, M. I., Waldron, S., and Malcolm, I. A.: Interpretation of homogeneity in  $\delta^{18}\text{O}$  signatures of stream water in a nested sub-catchment system in north-east Scotland, *Hydrol. Process.*, 22, 4767–4782, <https://doi.org/10.1002/hyp.7088>, 2008.
- Dupas, R., Jomaa, S., Musolff, A., Borchardt, D., and Rode, M.: Disentangling the influence of hydroclimatic patterns and agricultural management on river nitrate dynamics from sub-hourly to decadal time scales, *Sci. Total Environ.*, 571, 791–800, <https://doi.org/10.1016/j.scitotenv.2016.07.053>, 2016.
- 500 Dupas, R., Musolff, A., Jawitz, J. W., Rao, P. S. C., Jäger, C. G., Fleckenstein, J. H., Rode, M., and Borchardt, D.: Carbon and nutrient export regimes from headwater catchments to downstream reaches, *Biogeosciences*, 14, 4391–4407, <https://doi.org/10.5194/bg-14-4391-2017>, 2017.
- 505 Ehrhardt, S., Kumar, R., Fleckenstein, J. H., Attinger, S., and Musolff, A.: Trajectories of nitrate input and output in three nested catchments along a land use gradient, *Hydrol. Earth Syst. Sci.*, 23, 3503–3524, <https://doi.org/10.5194/hess-23-3503-2019>, 2019.
- Feng, X., Faiia, A. M., and Posmentier, E. S.: Seasonality of isotopes in precipitation: A global perspective, *J. Geophys. Res.*, 114, D08116, <https://doi.org/10.1029/2008JD011279>, 2009.
- Gupta, H. V., Kling, H., Yilmaz, K. K., and Martinez, G. F.: Decomposition of the mean squared error and NSE performance criteria: Implications for improving hydrological modelling, *J. Hydrol.*, 377, 80–91, <https://doi.org/10.1016/j.jhydrol.2009.08.003>, 2009.
- 510 Harman, C. J.: Time-variable transit time distributions and transport: Theory and application to storage-dependent transport of chloride in a watershed, *Water Resour. Res.*, 51, 1–30, <https://doi.org/10.1002/2014WR015707>, 2015.

- Harman, C. J.: Age-Ranked Storage-Discharge Relations: A Unified Description of Spatially Lumped Flow and Water Age in Hydrologic Systems, *Water Resour. Res.*, 55, 7143–7165, <https://doi.org/10.1029/2017WR022304>, 2019.
- 515 Heidbüchel, I., Yang, J., Musolff, A., Troch, P., Ferré, T., and Fleckenstein, J. H.: On the shape of forward transit time distributions in low-order catchments, *Hydrol. Earth Syst. Sci.*, 24, 2895–2920, <https://doi.org/10.5194/hess-24-2895-2020>, 2020.
- Heidbüchel, I., Troch, P. A., and Lyon, S. W.: Separating physical and meteorological controls of variable transit times in zero-order catchments, *Water Resour. Res.*, 49, 7644–7657, <https://doi.org/10.1002/2012WR013149>, 2013.
- Holvoet, K. M., Seuntjens, P., and Vanrolleghem, P. A.: Monitoring and modeling pesticide fate in surface waters at the catchment scale, *Ecol. Model.*, 209, 53–64, <https://doi.org/10.1016/j.ecolmodel.2007.07.030>, 2007.
- 520 Hrachowitz, M., Soulsby, C., Tetzlaff, D., Malcolm, I. A., and Schoups, G.: Gamma distribution models for transit time estimation in catchments: Physical interpretation of parameters and implications for time-variant transit time assessment, *Water Resour. Res.*, 46, W10536, <https://doi.org/10.1029/2010WR009148>, 2010.
- Hrachowitz, M., Soulsby, C., Tetzlaff, D., and Malcolm, I. A.: Sensitivity of mean transit time estimates to model conditioning and data availability, *Hydrol. Process.*, 25, 980–990, <https://doi.org/10.1002/hyp.7922>, 2011.
- 525 Hrachowitz, M., Savenije, H., Bogaard, T. A., Tetzlaff, D., and Soulsby, C.: What can flux tracking teach us about water age distribution patterns and their temporal dynamics?, *Hydrol. Earth Syst. Sci.*, 17, 533–564, <https://doi.org/10.5194/hess-17-533-2013>, 2013.
- Hrachowitz, M., Benettin, P., van Breukelen, B. M., Fovet, O., Howden, N. J. K., Ruiz, L van der Velde, Y., and Wade, A. J.: Transit times — the link between hydrology and water quality at the catchment scale, *WIREs Water*, 3, 629–657, <https://doi.org/10.1002/wat2.1155>, 2016.
- 530 Huang, T., Pang, Z., Li, J., Xiang, Y., and Zhao, Z.: Mapping groundwater renewability using age data in the Baiyang alluvial fan, NW, China, *Hydrogeol J.*, 25, 743–755, <https://doi.org/10.1007/s10040-017-1534-z>, 2017.
- Jasechko, S.: Global isotope hydrogeology — review, *Reviews of Geophysics*, 57, 835–965, <https://doi.org/10.1029/2018RG000627>, 2019.
- Jasechko, S., Wassenaar, L. I., and Mayer, B.: Isotopic evidence for widespread cold-season-biased groundwater recharge and young stream-flow across central Canada, *Hydrol. Process.*, 31, 2196–2209, <https://doi.org/10.1002/hyp.11175>, 2017.
- 535 Jiang, S., Jomaa, S., and Rode, M.: Modelling inorganic nitrogen leaching in nested mesoscale catchments in central Germany, *Ecohydro.*, 7, 1345–1362, <https://doi.org/10.1002/eco.1462>, 2014.
- Jing, M., Heße, F., Kumar, R., Kolditz, O., Kalbacher, T., and Attinger, S.: Influence of input and parameter uncertainty on the prediction of catchment-scale groundwater travel time distributions, *Hydrol. Earth Syst. Sci.*, 23, 171–190, <https://doi.org/10.5194/hess-23-171-2019>, 2019.
- 540 Kim, M. and Troch, P. A.: Transit time distributions estimation exploiting flow-weighted time: Theory and proof-of-concept, *Water Resour. Res.*, 56, e2020WR027186, <https://doi.org/10.1029/2020WR027186>, 2022.
- Kim, M., Pangle, L. A., Cardoso, C., Lora, M., Volkmann, T. H. M., Wang, Y., Harman, C. J., and Troch, P. A.: Transit time distributions and StorAge Selection functions in a sloping soil lysimeter with time-varying flow paths: Direct observation of internal and external transport variability, *Water Resour. Res.*, 52, 7105–7129, <https://doi.org/10.1002/2016WR018620>, 2016.
- 545 Kirchner, J. W.: Getting the right answers for the right reasons: Linking measurements, analyses, and models to advance the science of hydrology, *Water Resour. Res.*, 42, W03S04, <https://doi.org/10.1029/2005WR004362>, 2006.
- Kirchner, J. W.: Aggregation in environmental systems – Part I: Seasonal tracer cycles quantify young water fractions, but not mean transit times, in spatially heterogeneous catchments, *Hydrol. Earth Syst. Sci.*, 20, 279–297, <https://doi.org/10.5194/hess-20-279-2016>, 2016.
- Kirchner, J. W.: Quantifying new water fractions and transit time distributions using ensemble hydrograph separation: theory and benchmark tests, *Hydrol. Earth Syst. Sci.*, 23, 303–349, <https://doi.org/10.5194/hess-23-303-2019>, 2019.
- 550

- Kirchner, J. W., Feng, X., and Neal, C.: Fractal stream chemistry and its implications for contaminant transport in catchments, *Nature*, 403, 524–527, <https://doi.org/10.1038/35000537>, 2000.
- Kirchner, J. W., Feng, X., and Neal, C.: Catchment-scale advection and dispersion as a mechanism for fractal scaling in stream tracer concentrations, *J. Hydrol.*, 254, 82–101, [https://doi.org/10.1016/S0022-1694\(01\)00487-5](https://doi.org/10.1016/S0022-1694(01)00487-5), 2001.
- 555 Kirchner, J. W., Feng, X., Neal, C., and Robson, A. J.: The fine structure of water-quality dynamics: the (high-frequency) wave of the future, *Hydrol. Process.*, 18, 1353–1359, <https://doi.org/10.1002/hyp.5537>, 2004.
- Kolbe, T., de Dreuzy, J. R., Abbott, B. W., Aquilina, L., Babey, T., Green, C. T., et al.: Stratification of reactivity determines nitrate removal in groundwater, *Proceedings of the National Academy of Sciences*, 116(7), 2494–2499, <https://doi.org/10.1073/pnas.1816892116>, 2019.
- Kumar, R., Samaniego, L., and S., A.: The effects of spatial discretization and model parameterization on the prediction of extreme runoff characteristics, *J. Hydrol.*, 392, 54–69, <https://doi.org/10.1016/j.jhydrol.2010.07.047>, 2010.
- 560 Kumar, R., Samaniego, L., and Attinger, S.: Implications of distributed hydrologic model parameterization on water fluxes at multiple scales and locations, *Water Resour. Res.*, 49, 360–379, <https://doi.org/10.1029/2012WR012195>, 2013.
- Kumar, R., Heße, F., Rao, P. S. C., Musolff, A., Jawitz, J. W., Sarrazin, F., Samaniego, L., Fleckenstein, J. H., Rakovec, O., Thober, S., and Attinger, S.: Strong hydroclimatic controls on vulnerability to subsurface nitrate contamination across Europe, *Nature Communications*, 11, 6302, <https://doi.org/10.1038/s41467-020-19955-8>, 2020.
- 565 Le Gal La Salle, C., Marlin, C., Leduc, C., Taupin, J. D., Massault, M., and Favreau, G.: Renewal rate estimation of groundwater based on radioactive tracers (<sup>3</sup>H, <sup>14</sup>C) in an unconfined aquifer in a semi-arid area, Iullemeden Basin, Niger, *J. Hydrol.*, 254, 145–156, [https://doi.org/10.1016/S0022-1694\(01\)00491-7](https://doi.org/10.1016/S0022-1694(01)00491-7), 2001.
- Leu, C., Singer, H., Stamm, C., Muller, S. R., and Schwarzenbach, R. P.: Simultaneous Assessment of Sources, Processes, and Factors Influencing Herbicide Losses to Surface Waters in a Small Agricultural Catchment, *Environ. Sci. Technol.*, 38, 3827–3834, <https://doi.org/10.1021/es0499602>, 2004.
- 570 Lutz, S., van Meerveld, H. J., Waterloo, M. J., Broers, H. P., and van Breukelen B. M.: A model-based assessment of the potential use of compound-specific stable isotope analysis in river monitoring of diffuse pesticide pollution, *Hydrol. Earth Syst. Sci.*, 17, 4505–4524, <https://doi.org/10.5194/hess-17-4505-2013>, 2013.
- 575 Lutz, S. R., van der Velde, Y., Elsayed, O. F., Imfeld, G., Lefrancq, M., Payraudeau, S., and van Breukelen, B. M.: Pesticide fate on catchment scale: conceptual modelling of stream CSIA data, *Hydrol. Earth Syst. Sci.*, 21, 5243–5261, <https://doi.org/10.5194/hess-21-5243-2017>, 2017.
- Lutz, S. R., Krieg, R., Müller, C., Zink, M., Knöller, K., Samaniego, L., and Merz, R.: Spatial patterns of water age: using young water fractions to improve the characterization of transit times in contrasting catchments, *Water Resour. Res.*, 54, 4767–4784, <https://doi.org/10.1029/2017WR022216>, 2018.
- 580 Lutz, S. R., Ebeling, P., Musolff, A., Nguyen, T. V., Sarrazin, F. J., Van Meter, K. J., Basu, N. B., Fleckenstein, J. H., Attinger, S., and Kumar, R.: Pulling the rabbit out of the hat: Unravelling hidden nitrogen legacies in catchment-scale water quality models, *Hydrol. Processes*, 36, e14682, <https://doi.org/10.1002/hyp.14682>, 2022.
- McDonnel, J. J., McGuire, K., Aggarwal, P., Beven, K. J., Biondi, D., Destouni, G., et al.: How old is streamwater? Open questions in catchment transit time conceptualization, modelling and analysis, *Hydrol. Process.*, 24, 1745–1754, <https://doi.org/10.1002/hyp.7796>, 2010.
- 585 McDonnel, J. J., McGuire, K. J. and McDonnel, J. J.: A review and evaluation of catchment transit time modeling, *J. Hydrol.*, 330, 543–563, <https://doi.org/10.1016/j.jhydrol.2006.04.020>, 2006.

- McKay, M. D., Beckman, R. J., and Conover, W. J.: A Comparison of Three Methods for Selecting Values of Input Variables in the Analysis  
590 of Output from a Computer Code, *Technometrics*, 21, 239–245, <https://doi.org/10.2307/1268522>, 1979.
- Morgenstern, U., Daughney, C. J., Leonard, G., Gordon, D., Donath, F. M., and Reeves, R.: Using groundwater age and hydrochemistry to  
understand sources and dynamics of nutrient contamination through the catchment into Lake Rotorua, New Zealand, *Hydrol. Earth Syst.  
Sci.*, 19, 803–822, <https://doi.org/10.5194/hess-19-803-2015>, 2015.
- Nguyen, T. V., Kumar, R., Lutz, S. R., Musolff, A., Yang, J., and Fleckenstein, J. H.: Modeling Nitrate Export From a Mesoscale Catchment  
595 Using StorAge Selection Functions, *Water Resour. Res.*, 57, e2020WR028490, <https://doi.org/10.1029/2020WR028490>, 2021.
- Nguyen, T. V., Sarrazin, F. J., Ebeling, P., Musolff, A., Fleckenstein, J. H., and Kumar, R.: Toward Understanding of Long-Term Nitrogen  
Transport and Retention Dynamics Across German Catchments, *Geophysical Research Letters*, 49, e2022GL100278, 2022.
- Niemi, A. J.: Residence time distributions of variable flow processes, *The International Journal of Applied Radiation and Isotopes*, 28(10),  
855–860, [https://doi.org/10.1016/0020-708X\(77\)90026-6](https://doi.org/10.1016/0020-708X(77)90026-6), 1977.
- 600 Opazo, T., Aravena, R., and Parker, B.: Nitrate distribution and potential attenuation mechanisms of a municipal water supply bedrock  
aquifer, *Applied Geochemistry*, 73, 157–168, <https://doi.org/10.1016/j.apgeochem.2016.08.010>, 2016.
- Queloz, P., Carraro, L., Benettin, P., Botter, G., Rinaldo, A., and Bertuzzo, E.: Transport of fluorobenzoate tracers in a vegetated hydrologic  
control volume: 2. Theoretical inferences and modeling., *Water Resour. Res.*, 51, 2793–2806, <https://doi.org/10.1002/2014WR016508>,  
2015.
- 605 Rinaldo, A. and Marani, M.: Basin Scale Model of Solute Transport, *Water Resour. Res.*, 23, 2107–2118,  
<https://doi.org/10.1029/WR023i011p02107>, 1987.
- Rinaldo, A., Botter, G., Bertuzzo, E., Uccelli, A., Settin, T., and Marani, M.: Transport at basin scales: 1. Theoretical framework, *Hydrol.  
Earth Syst. Sci.*, 10, 19–29, <https://doi.org/10.5194/hess-10-19-2006>, 2006.
- Rinaldo, A., Benettin, P., Harman, C. J., Hrachowitz, M., McGuire, K. J., van der Velde, Y., et al.: Storage selection functions:  
610 A coherent framework for quantifying how catchments store and release water and solutes, *Water Resour. Res.*, 51, 4840–4847,  
<https://doi.org/10.1002/2015WR017273>, 2015.
- Rodriguez, N. B., McGuire, K. J., and Klaus, J.: Time-Varying Storage–Water Age Relationships in a Catchment With a Mediterranean  
Climate, *Water Resour. Res.*, 54, 3988–4008, <https://doi.org/10.1029/2017WR021964>, 2018.
- Rodriguez, N. B., Pfister, L., Zehe, E., and Klaus, J.: A comparison of catchment travel times and storage deduced from deuterium and tritium  
615 tracers using StorAge Selection functions, *Hydrol. Earth Syst. Sci.*, 25, 401–428, <https://doi.org/10.5194/hess-25-401-2021>, 2021.
- Rodríguez-Cruz, M. S., Jones, J. E., and Bending, G. D.: Field-scale study of the variability in pesticide biodegradation with soil depth and its  
relationship with soil characteristics, *Soil Biology and Biochemistry*, 38, 2910–2918, <https://doi.org/10.1016/j.soilbio.2006.04.051>, 2006.
- Samaniego, L., Kumar, R., and Attinger, S.: Multiscale parameter regionalization of a grid-based hydrologic model at the mesoscale, *Water  
Resour. Res.*, 46, W05523, <https://doi.org/10.1029/2008WR007327>, 2010.
- 620 Schoups, G., van de Giesen, N. C., and Savenije, H. H. G.: Model complexity control for hydrologic prediction, *Water Resour. Res.*, 44,  
W00B03, <https://doi.org/10.1029/2008WR006836>, 2008.
- Seeger, S. and Weiler, M.: Reevaluation of transit time distributions, mean transit times and their relation to catchment topography, *Hydrol.  
Earth Syst. Sci.*, 18, 4751–4771, <https://doi.org/10.5194/hess-18-4751-2014>, 2014.
- Soulsby, C. and Tetzlaff, D.: Towards simple approaches for mean residence time estimation in ungauged basins using tracers and soil  
625 distributions, *J. Hydrol.*, 363, 60–74, <https://doi.org/10.1016/j.jhydrol.2008.10.001>, 2008.

- Stewart, M. K., Morgenstern, U., and McDonnell, J. J.: Truncation of stream residence time: How the use of stable isotopes has skewed our concept of streamwater age and origin, *Hydrol. Process.*, 24, 1646–1659, <https://doi.org/10.1002/hyp.7576>, 2010.
- Stewart, M. K., Morgenstern, U., McDonnell, J. J., and Pfister, L.: The ‘hidden streamflow’ challenge in catchment hydrology: A call to action for stream water transit time analysis, *Hydrol. Process.*, 26, 2061–2066, <https://doi.org/10.1002/hyp.9262>, 2012.
- 630 Stockinger, M. P., Lücke, A., McDonnell, J. J., Diekkrüger, B., Vereecken, H., and Bogena, H. R.: Interception effects on stable isotope driven streamwater transit time estimates, *Geophys. Res. Lett.*, 42, 5299–5308, <https://doi.org/doi:10.1002/2015GL064622>, 2015.
- Sutanudjaja, E. H., Van Beek, R., Wanders, N., Wada, Y., Bosmans, J. H. C., et al.: PCR-GLOBWB 2: a 5 arcmin global hydrological and water resources model, *Geosci. Model Dev.*, 11, 2429–2453, <https://doi.org/10.5194/gmd-11-2429-2018>, 2018.
- Svensson, T., Lovett, G. M., and Likens, G. E.: Is chloride a conservative ion in forest ecosystems?, *Biogeochemistry*, 107, 125–134, <https://doi.org/10.1007/s10533-010-9538-y>, 2012.
- 635 Tetzlaff, D., Piovano, T., A., P., Smith, A., K., C. S., Marsh, P., Wookey, P. A., Street, L. E., and Soulsby, C.: Using stable isotopes to estimate travel times in a data-sparse Arctic catchment: Challenges and possible solutions, *Hydrol. Process.*, 32, 1936–1952, <https://doi.org/10.1002/hyp.13146>, 2018.
- Thiemig, V., Rojas, R., Zombrano-Bigiarini, M., and De Roo, A.: Hydrological evaluation of satellite-based rainfall estimates over the Volta and Baro-Akobo Basin, *J. Hydrol.*, 499, 324–338, <https://doi.org/10.1016/j.jhydrol.2013.07.012>, 2013.
- Van der Velde, Y., De Rooij, G. H., Rozemeijer, J. C., Van Geer, F. C., and Broers, H. P.: Nitrate response of a lowland catchment: On the relation between stream concentration and travel time distribution dynamics, *Water Resour. Res.*, 46, W11534, <https://doi.org/10.1029/2010WR009105>, 2010.
- van der Velde, Y., Torfs, P. J. J. F., van der Zee, S. E. A. T. M., and Uijlenhoet, R.: Quantifying catchment-scale mixing and its effect on time-varying travel time distributions, *Water Resour. Res.*, 48, W06536, <https://doi.org/10.1029/2011WR011310>, 2012.
- 645 Van Meter, K. J., Basu, N. B., and Van Cappellen, P.: Two centuries of nitrogen dynamics: legacy sources and sinks in the Mississippi and Susquehanna river basins, *Global Biogeochemical Cycles*, 31, 2–23, <https://doi.org/10.1002/2016GB005498>, 2017.
- Visser, A., Broers, H. P., Purtschert, R., Sültenfuß, J., and de Jonge, M.: Groundwater age distributions at a public drinking water supply well field derived from multiple age tracers (85Kr, 3H/3He, and 39Ar), *Water Resour. Res.*, 49, 7778–7796, <https://doi.org/10.1002/2013WR014012>, 2013.
- 650 Visser, A., Thaw, M., Deinhart, A., Bibby, R., Safeeq, M., Conklin, M., Esser, B., and van der Velde, Y.: Cosmogenic isotopes unravel the hydrochronology and water storage dynamics of the Southern Sierra critical zone, *Water Resour. Res.*, 55, 1429–1450, <https://doi.org/10.1029/2018WR023665>, 2019.
- von Freyberg, J., Studer, B., and Kirchner, J. W.: A lab in the field: high-frequency analysis of water quality and stable isotopes in stream water and precipitation, *Hydrol. Earth Syst. Sci.*, 21, 1721–1739, <https://doi.org/10.5194/hess-21-1721-2017>, 2017.
- 655 von Freyberg, J., Allen, S. T., Seeger, S., Weiler, M., and Kirchner, J. W.: Sensitivity of young water fractions to hydro-climatic forcing and landscape properties across 22 Swiss catchments, *Hydrol. Earth Syst. Sci.*, 22, 3841–3861, <https://doi.org/10.5194/hess-22-3841-2018>, 2018.
- von Freyberg, J., Rücker, A., Zappa, M., Schlumpf, A., Studer, B., and Kirchner, J. W.: Four years of daily stable water isotope data in stream water and precipitation from three Swiss catchments, *Sci Data*, 9, 46, <https://doi.org/10.1038/s41597-022-01148-1>, 2022.
- 660 Wang, S., Hrachowitz, M., Schoups, G., and Stumpp, C.: Stable water isotopes and tritium tracers tell the same tale: No evidence for underestimation of catchment transit times inferred by stable isotopes in SAS function models, *Hydrol. Earth Syst. Sci. Discuss.* [preprint], in review, <https://doi.org/10.5194/hess-2022-400>, 2022.

- 665 Wilusz, D. C., Harman, C. J., and Ball, W. P.: Sensitivity of Catchment Transit Times to Rainfall Variability Under Present and Future  
Climates, *Water Resour. Res.*, 53, 10 231–10 256, <https://doi.org/10.1002/2017WR020894>, 2017.
- Winter, C., Lutz, S. R., Musolff, A., Kumar, R. Weber, M., and Fleckenstein, J. H.: Disentangling the Impact of Catchment  
Heterogeneity on Nitrate Export Dynamics From Event to Long-Term Time Scales, *Water Resour. Res.*, 57, e2020WR027 992,  
<https://doi.org/10.1029/2020WR027992>, 2020.
- 670 Winter, C., Nguyen, T. V., Musolff, A., Lutz, S. R., Rode, M., Kumar, R., , and Fleckenstein, J. H.: Droughts can reduce the nitrogen retention  
capacity of catchments, *Hydrol. Earth Syst. Sci.*, 27, 303—318, <https://doi.org/10.5194/hess-27-303-2023>, 2023.
- Wollschläger, U., Attinger, S., Borchardt, D., Brauns, M., Cuntz, M., Dietrich, P., et al.: The Bode hydrological observatory: a platform for  
integrated, interdisciplinary hydro-ecological research within the TERENO Harz/Central German Lowland Observatory, *Environmental  
Earth Sciences*, 76, 29, <https://doi.org/10.1007/s12665-016-6327-5>, 2017.
- 675 Xu, G., Magen, H., Tarchitzky, J., and Kafkafi, U.: Advances in Chloride Nutrition of Plants, *Adv. Agron.*, 68, 97–150,  
[https://doi.org/10.1016/S0065-2113\(08\)60844-5](https://doi.org/10.1016/S0065-2113(08)60844-5), 1999.
- Zink, M., Kumar, R., Cuntz, M., and Samaniego, L.: A high-resolution dataset of water fluxes and states for Germany accounting for  
parametric uncertainty, *Hydrol. Earth Syst. Sci.*, 21, 1769–1790, <https://doi.org/10.5194/hess-21-1769-2017>, 2017.